Clinica Chimica Acta 494 (2019) 64–70

Contents lists available at ScienceDirect

Clinica Chimica Acta

journal homepage: www.elsevier.com/locate/cca

Homozygosity mapping and whole exome sequencing reveal a novel *ERCC8* mutation in a Chinese consanguineous family with unique cerebellar ataxia

Danyan Zhang[a,b,1], Limeng Dai[a,1], Zhenhua Zhou[c], Jun Hu[c], Yun Bai[a,*], Hong Guo[a,*]

[a] *Department of Medical Genetics, College of Basic Medicine, Army Medical University (Third Military Medical University), 30#, Gaotanyan St., Shapingba District, Chongqing 400038, PR China*

[b] *Key Laboratory of Birth Defects and Reproductive Health of National Health and Family Planning Commission (Chongqing Key Laboratory of Birth Defects and Reproductive Health, Chongqing Population and Family Planning Science and Technology Research Institute, 18#, Honghuang Road, Jiangbei District, Chongqing 400020, PR China*

[c] *Department of Neurology, Southwest Hospital, Army Medical University (Third Military Medical University), 30#, Gaotanyan St., Shapingba District, Chongqing 400038, PR China*

ARTICLE INFO

Keywords:
Spinocerebellar ataxia
ERCC8
Homozygosity mapping
Whole exome sequencing
Cockayne syndrome type A

ABSTRACT

Background: A consanguineous Chinese family was affected by an apparently novel autosomal recessive disorder characterized by cerebellar ataxia, cutaneous photosensitivity, and mild intellectual disability.

Methods: The family was evaluated by homozygosity mapping, haplotype analysis, whole exome sequencing, and candidate gene mutation screening to identify the disease-associated gene and mutation. Bioinformatics methods were used to predict the functional significance of the mutated gene product. *ERCC8* mutations and phenotypes were examined.

Results: All three patients presented cerebellar ataxia, cutaneous photosensitivity, and mild intellectual disability. Whole genome and candidate region linkage analysis in the consanguineous family revealed a maximum logarithm of the odds score at 5q12.1. This homozygous region was confirmed by homozygosity mapping. The pathogenic missense mutation p.Gly257Arg affecting an evolutionary highly conserved amino acid was identified in *ERCC8* at 5q12.1. Integrated application of whole exome sequencing and homozygosity mapping is an efficient approach for gene mapping and mutation identification in consanguineous families.

Conclusions: We identified a novel *ERCC8* mutation and new unique disease phenotype. These results also confirmed the genotype-phenotype relationship between mutations in *ERCC8* and clinical findings.

1. Introduction

Autosomal recessive cerebellar ataxias constitute a highly heterogeneous group of neurodegenerative disorders, which mainly affect the nervous system. Recessive ataxias may present as a pure cerebellar syndrome or are associated with neurological symptoms or extra neurological symptoms [1]. The main clinical features of these disorders include staggering gait, upper limb dysmetria, dysarthria, and dysphagia. Other common features are intellectual disability, dystonia, tremor, chorea, peripheral neuropathy, and nystagmus.

According to the OMIM database (http://www.omim.org/), intellectual disability is a common feature of recessive ataxia, such as autosomal recessive spinocerebellar ataxia (SCAR type 2, 4, 10, 14, 17, 18, 20, 21, 22, 23) [2–4]. However, an association between recessive ataxia and photosensitive dermatitis is uncommon, and may be observed in diseases related to DNA damage repair genes, such as xeroderma pigmentosum (XPF; groups A, B, D, F, and G) and Cockayne syndrome (CS; types A and B) [5,6]. The co-occurrence of recessive ataxia, skin photosensitivity, and intellectual disability has been described in a few rare syndromes, including CS and XPF [7,8]. CS is characterized by a variety of clinical features, including progressive growth failure, microcephaly, cutaneous photosensitivity, progeroid appearance, flexion contractures of joints, delayed neural development, and severe progressive neurologic degeneration resulting in cognitive

Abbreviations: ACMG, American College of Medical Genetics and Genomics; CADD, Combined Annotation Dependent Depletion; CS-A, Cockayne syndrome type A; MAF, Minimum Allele Frequency; MRI, Magnetic Resonance Imaging; NER, nucleotide excision repair; ROH, Runs of Homozygosity; SCAR, Autosomal Recessive Spinocerebellar Ataxia; SNP, single nucleotide polymorphism; SNVs, Single Nucleotide variants; UVSS-2, UV-sensitive syndrome 2; XP, Xeroderma Pigmentosum

* Corresponding authors at: 30#, Gaotanyan St., Shapingba District, Chongqing 400038, PR China
E-mail addresses: yunbai@tmmu.edu.cn (Y. Bai), guohong02@gmail.com (H. Guo).

[1] Danyan Zhang and Limeng Dai contributed equally to this work.

https://doi.org/10.1016/j.cca.2019.03.1609
Received 30 January 2019; Received in revised form 6 March 2019; Accepted 10 March 2019
Available online 12 March 2019
0009-8981/ © 2019 Published by Elsevier B.V.

defects, pigmentary retinopathy, cataracts, sensorineural deafness, feeding difficulties, and premature death [6]. XPF is a mild form of XP, which is characterized by sun sensitivity and increased skin sensitivity to UV light, as well as an increased risk of skin cancer. Some patients with XPF develop neurologic impairment or growth defects and are thus classified as having CS [9].

We report a new autosomal recessive Cockayne-like syndrome, characterized by a combination of spinocerebellar ataxia, skin photosensitivity, and intellectual disability. We identified a homozygous missense mutation in *ERCC8* (MIM 609412) in a consanguineous family by whole exome sequencing combined with genome-wide homozygosity mapping.

2. Materials and methods

2.1. Research subjects

The study was performed with the approval of the Ethics Committee of Army Medical University (Chongqing, China). Written informed consent was obtained from the family members and healthy controls to participate in this study. The participants in the family in this study were identified and enrolled at Southwest Hospital, Army Medical University. Both patients and normal controls underwent physical examination in the Department of Neurology. DNA samples were collected from affected family members, their unaffected siblings, and their parents between October 2013 and September 2014. The 150 unaffected controls were defined healthy individuals from physical examination population at Southwest Hospital during 2013 to 2016. The quantity and quality of DNA was determined by using a NANODROP 1000 (Thermo Fisher Scientific, Waltham, MA, USA).

2.2. Linkage analysis and homozygosity mapping

Genome wide scanning was first conducted to localize the candidate regions linked to the disease phenotype. Genotyping was performed on the Genome-Wide Human SNP Array 6.0 (Affymetrix, Santa Clara, CA, USA). This array consists of 900 K single-nucleotide polymorphisms (SNPs) with a mean distance of 4 kb. Chips and data were processed on the Affymetrix platform with Command Console Software. SNP genotypes were called using the Affymetrix BRLMM algorithm in Genotyping Console 3.0 Software (Affymetrix). We performed multipoint linkage analysis using MERLIN software (http://www.sph.umich.edu/csg/abecasis/Merlin/) assuming a fully penetrant recessive model and disease allele frequency of 0.001.

The genotyping data were used to define the runs of homozygosity for every patient using PLINK. We defined homozygous regions as those with 50 consecutive homozygous SNPs, irrespective of the total length of the genomic region, allowing for one mismatch; only SNPs with a minimum allele frequency > 0.3 were included in the analysis. The runs of homozygosity were further defined as genomic regions demarcated by the first encountered heterozygous SNP flanking each established homozygous region. The areas of homozygosity were confirmed by genotyping of microsatellite markers and high-resolution haplotype analysis in the family. Two-point logarithm of the odds (LOD) scores were calculated using the MLINK program in the FASTLINK package with the same parameters used above.

2.3. Exome sequencing

The genomic DNA of the patients was fragmented to generate 200–300-base pair fragments using Covaris S2 (Covaris, Massachusetts, USA) according to the manufacturer's instructions. Paired-end libraries were prepared following the Illumina library preparation protocol. The exome was captured using the SureSelect Human All Exons Plus kit (Agilent). Paired-end sequencing was carried out on an Illumina HiSeq 2000 sequencer (Illumina, San Diego, CA, USA) with a read length of 2×100 bp, average depth of at least $50\times$, coverage at least 98.5%, fraction of target covered over $20\times$ at least 90% for each sample. Raw image files were processed by the Illumina Pipeline for base calling using default parameters. Primary data were in fastq format after image analysis and base calling was conducted using the Illumina Pipeline. The data were filtered to generate “clean reads” by removing adapters and low-quality reads. The raw results were analysed by using a standard pipeline that utilized published algorithms in a sequential manner. Sequencing reads were mapped to the reference human genome version hg19 (http://genome.ucsc.edu/). Variant analysis was performed using SOAPsnp software (V1.05) and Samtools (V1.5) for SNPs and indels, respectively. All SNPs were identified by using the NCBI dbSNP, HapMap, 1000 human genome dataset (http://www.1000genomes.org/), the Exome Aggregation Consortium (ExAC), the Chinese Millionome Database (CMDB) (https://db.cngb.org/cmdb/), local database of BGI (Shenzhen, China) and the database of Chigene Translational Medical Research Center (Beijing, China).

2.4. Sequencing of ERCC8

Variants identified by exome sequencing were confirmed by Sanger DNA sequencing, and familial segregation analyses were performed as extensively as possible. The software Primer3 was used to design primers to amplify whole exons and exon-intron boundaries of *ERCC8*. Conditions and the primer pairs for PCR are available upon request. PCR products were checked on 2% agarose gel electrophoresis and purified with a purification kit (Tiangen, Beijing, China). Purified PCR products were directly sequenced in both the forward and reverse directions on an ABI 3130 genetic analyser (Applied Biosystems, Foster City, CA, USA) according to the manufacturer's instructions. DNA sequences were analysed using the vector NTI 11.0 software package. The DNA mutation numbering system we used is based on cDNA sequences with +1 corresponding to the A of the ATG translation initiation codon in the reference sequence, according to journal guidelines (www.hgvs.org/mutnomen).

2.5. Functional significance prediction

Several online prediction software programs were used to predict the functional significance of the mutation, including PolyPhen 2 (http://genetics.bwh.harvard.edu/pph2) and SIFT (http://sift.jcvi.org). MutationTaster (http://www.mutationtaster.org/) is an important online software designed to predict the damaging effects of alternative amino acids. Combined Annotation Dependent Depletion (CADD, https://cadd.gs.washington.edu/) is a tool for scoring the damaging effects of single-nucleotide variants as well as insertion/deletions variants in the human genome. The CADD score combines information from 63 different annotations by using a support vector machine classifier. The score ranges from 1 to 99, with a higher score indicating greater deleteriousness. I-Mutant v2.0 (http://folding.biofold.org/i-mutant/i-mutant2.0.html) is a predictor of protein stability changes upon mutations.

2.6. Review of ERCC8 mutations

ERCC8 encodes CSA, a WD40 repeat protein belonging to the Swi2/Snf2 family. Isoform 1 (NP_000073.1) contains 361 amino acids, which is the largest functional protein. We reviewed *ERCC8* mutations to better understand the mutation spectrum of *ERCC8* and genotype-phenotype correlations.

3. Results

3.1. Clinical report

The proband (IV9) is a man from the southwest of China. He was

born to a consanguineous Chinese family (Fig. 1A) by normal vaginal delivery without any abnormalities in height, weight, and head circumference. The parents noted the onset of cutaneous photosensitivity at the age of 12 months. After 2 years old, he exhibited mild intellectual disability, delay in mental milestones, learning difficulties, difficulty in finding directions, and poor memory. However, he completed 12 years of education. Two years ago, the proband presented several motor symptoms, including four-limb ataxia that started as lower limb tremor and mildly increased deep tendon reflexes. Additionally, he temporarily suffers from myoclonic movements. At the age of 36 years, he was referred to the Southwest hospital and underwent a detailed physical check-up and genetic counselling. The clinical phenotypes were evaluated by a neurologist, general practitioner, and clinical geneticist. The proband had a normal height, weight, hearing, vision, and normal facial features. He often has skin redness on his body following exposure to the sun (Fig. S1). The oldest sister (IV1) and brother (IV3) of the proband had similar but milder symptoms, while the other family members were normal. Karyotype analysis revealed a normal male C-banded karyotype. Additionally, brain magnetic resonance imaging (MRI) of the proband revealed moderate and mild atrophy in the cerebellum and brainstem. There were also positive findings in the MRI results of IV1 and IV3 (Fig. 1B), which showed mild cerebral atrophy and cerebellar vermis dysplasia. The MRI results were normal in the healthy family members, including III3, IV5, and IV7 (Fig. 1B).

3.2. Disease gene linkage analysis and homozygosity mapping

The family was analysed by genome-wide linkage analysis, which revealed five chromosomal segments with LOD scores over 2.4, including 1p13.3-p21.1, 3p22.2-p22.3, 5q11.2-q13.2, 11q22.3, and 17q22-q23.2. Homozygosity mapping confirmed the five linked regions (Fig. 2). To further define the disease gene linkage region, microsatellite markers near the five candidate regions were selected and genotyped for high-resolution haplotype analysis of the family. Ultimately, the haplotype in the 5q11.2-q13.2 region was found to cosegregate with the disease phenotype in this family.

3.3. Identification of the pathogenic variant

Whole exome sequencing of the subject (IV9) was performed to identify the cause of pathogenesis for this uncertain disorder. In general, the test platform examined > 98% of the targeted regions with a sensitivity of > 99%. The average sequencing depth on the target was 74.5, with 94.5% of the targeted region covered with a minimum read depth of 10, providing sufficient depth to call SNPs and insertion/deletion (indels). In total, > 110 K annotated variants were identified with a hetero/homo ratio of 1.37. Calls with minor allele frequencies > 0.5% in the 1000 genomes dataset were filtered.

According to the American College of Medical Genetics and Genomics variants interpretation standards, homozygosity mapping results, and large sample exome information of Chinese from CMDB, local database of BGI and Chigene Translational Medical Research Center, 5 homozygous variants were chosen. When prioritizing presumed loss-of-function sequence alterations and clinical phenotypes, we identified a rare novel homozygous mutation in *ERCC8* (MIM #609412), c.769G > A, p.Gly257Arg (numbered according to NM_000082.3), that has been submitted to clinVar (www.ncbi.nlm.nih.gov/clinvar/) with the accessible no. SUB4753668.

3.4. Confirmation of the pathogenicity of the variant

This variant was in the largest region of homozygosity (5q11.2-q13.2) and was verified by Sanger sequencing (Fig. 3a). No potentially pathogenic variants were identified by exome sequencing in any genes currently known to be associated with ataxia or intellectual disability-associated genes. The proband's older sister (IV1) and older brother (IV3) were also found to harbour the *ERCC8* variant in the homozygous state. Both the father (III4), mother (III5), one unaffected sibling (IV5), and offspring of the patients (V1, V2, and V5) were heterozygous for the variant. We screened *ERCC8* by Sanger sequencing in 150 normal controls. No pathogenic variants were identified, particularly at the site c.769G.

The *ERCC8* p.Gly257Arg variant falls within the highly conserved WD-5 domain (Figs. 3b and 4). To predict the pathogenicity of the novel mutation, we used different bioinformatics software and approaches. The following results support the disease-causing feature of the mutation. PolyPhen 2, SIFT, and MutationTaster predicted that this variation was damaging or disease-causing. I-Mutant v2.0 revealed that protein stability is decreased when Gly is changed to Arg at 257. As shown in Fig. 3b, comparative amino acid alignment of the CSA protein across Kingdoms using Multiple Sequence Alignment Program revealed that this amino acid has been highly conserved during evolution. CADD

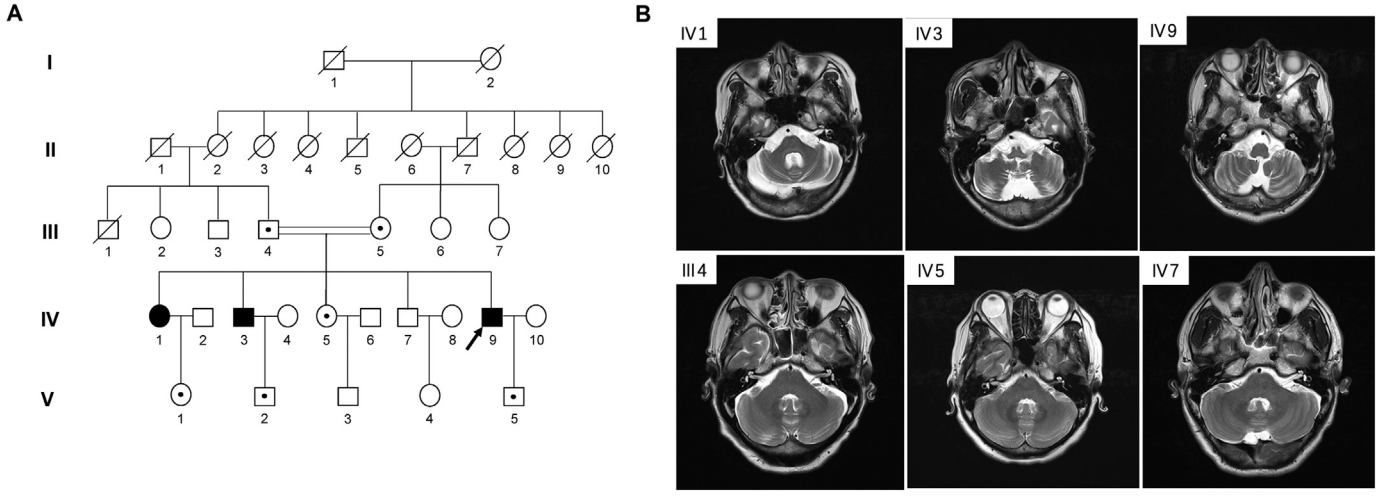

Fig. 1. (A). Pedigree analysis of families in the study. Squares and circles indicate men and women, respectively. The symbols in black represent the affected members. The obligate carriers are marked with solid circles. The arrow indicates the proband. The square with a line indicated a deceased individual. The pedigree shows a recessive consanguineous family. (B). Magnetic resonance imaging (MRI) scans of the brain. The top three panels show T2-weighted brain MRI of the proband (IV9), affected sister (IV1), and affected brother (IV3). The bottom three panels show T2-weighted brain MRI of the father (III3), normal sister (IV5), and normal brother (IV7).

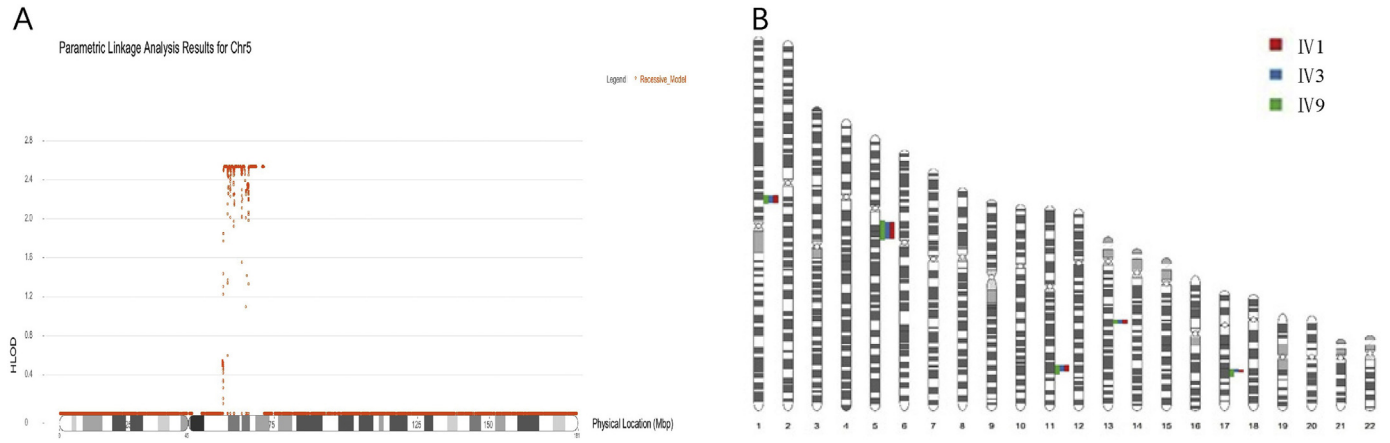

Fig. 2. Genome wide linkage analysis and homozygosity mapping results of the family. Panel A shows the chromosomal region 5q11.2-q13.2 with LOD score over 2.4. Panel B shows that 5q11.2-q13.2 is the largest homozygous region. The coloured bars indicate the length of the homozygous regions in the three patients (IV1, IV3, and IV9).

showed a score of 29.6 for this change, indicating its deleterious effects. Based on these data, the p.Gly257Arg variant in WD-5 of *ERCC8* is likely pathogenic in the patients in the family.

3.5. Mutation review and genotype-phenotype correlations

To date, including the p.Gly257Arg mutation in this Cockayne-like syndrome family, 58 different mutations in *ERCC8* have been reported in CS type A (CS-A) and UV-sensitive syndrome 2 (UVSS-2) patients (Fig. 4), which spread over nearly all 12 exons of *ERCC8*. Only one missense mutation, p.W361C, was reported to be related to UVSS-2 patients.

Of all 58 pathogenic genetic variants, *ERCC8* contains 18 missense mutations, 16 splicing mutations, 11 deletions (including 2 gross deletions), 6 nonsense mutations, 4 insertions, 2 rearrangements, and 1 indel (Table S1). Mutations in exons 4, 5, 7, and 11 were found in most CSA families with *ERCC8* mutations (Fig. S2). Point mutations are indicated above the CSA linear structure (Fig. 4) with the novel mutation p.Gly257Arg marked by #. CSA comprises a seven-bladed WD40 propeller. All missense mutations, except for E374D, affect residues in WD40 repeats. There is a particularly high concentration of missense mutations at WD-4 and WD-5 (around amino acids 200 and 270).

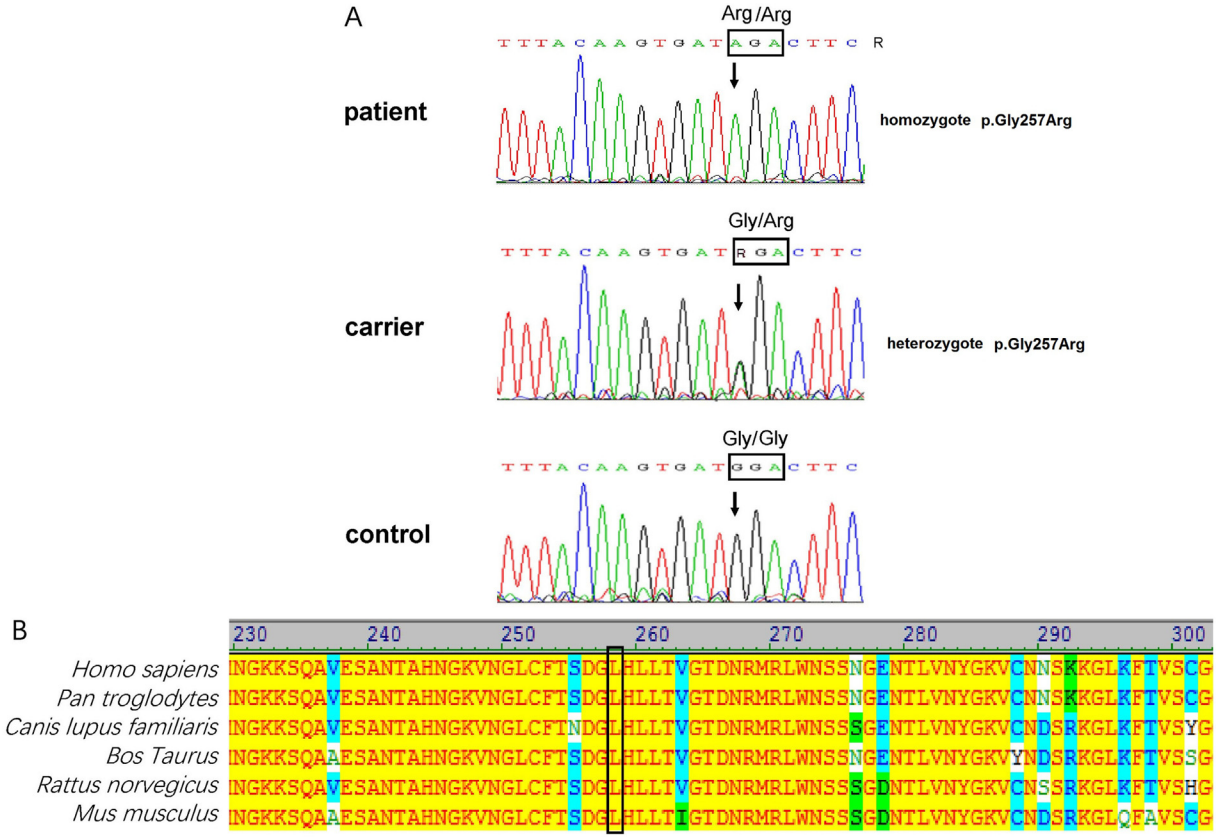

Fig. 3. Chromatograms of DNA sequence showing mutation in *ERCC8* genomic DNA. (A). The DNA sequence chromatogram of the patient indicates a homozygous missense mutation c.769G > A, which resulted in substitution of Glycine (Gly, G) to arginine (Arg, R) at codon 257 (p.Gly257Argp). The healthy carriers are heterozygous for the variant. (B). Conservation analysis showed that this novel missense mutation affected a highly conserved amino acid.

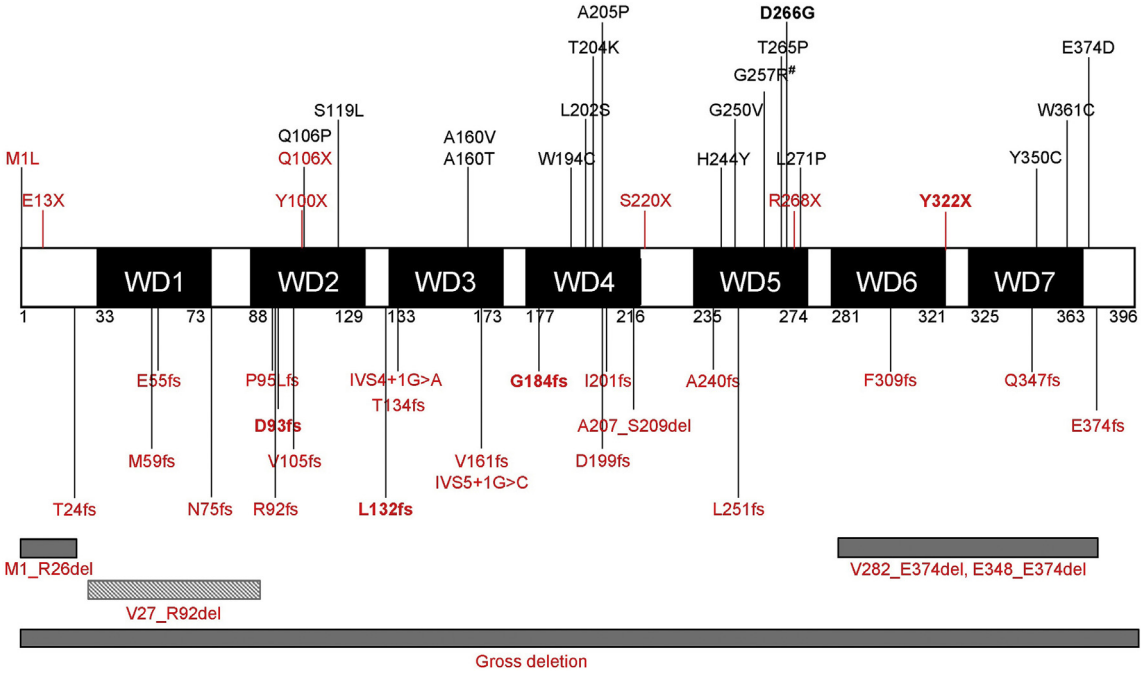

Fig. 4. Summary of the mutations identified in CSA in different ethnic groups. The missense and nonsense mutations are indicated above the protein, while the insertion, deletion, splicing, and rearrangement mutations are indicated below. WD1–WD7 indicate the seven WD40 domains of the ERCC8 protein according to NP_000073.1. Mutation identified in this study is marked by #. The five founder mutations are indicated in bold.

According to previous CSA cohort studies [10–12], several variants may be founder mutations, which are only found in a relatively limited geographical location. These founder mutations are indicated in bold (Fig. 4), including exon4 rearrangement in an East Asian population, c.394delTTACA in a Chinese population, c.966C > A in an Arabic population, c.551-1G > A in an African population, and c.797A > G in a European population.

The phenotype of our family is an intermediate phenotype between UVSS-2 and typical CS-A caused by *ERCC8* mutations, which is important for genotype-phenotype analysis. Homozygous missense mutations were rare in *ERCC8* that only p.W361C was reported to be related to UVSS-2 in previous studies. In our study, the phenotype of homozygous p.G257R presented atypical CS-A, which was related cerebellar ataxia, cutaneous photosensitivity, and mild intellectual disability. In the patients with typical CS-A, compound heterozygous mutations (a missense mutation with a nonsense/ frameshift mutation) were often reported. These data suggested that the *ERCC8* phenotype was continuous, and it may relate the lost dose of protein function. Mutation only involved C-terminal (WD7) of protein (p.W361C) causes UVSS-2, while mutation involving the high concentration of middle part of protein (WD5) could lead to atypical CS-A. As the level of protein dose loss increased, such as patient carried a missense mutation and a nonsense/frameshift mutation, will present a more serious disease phenotype, showing a typical CS-A.

4. Discussion

In this study, we reported an atypical CS and discovered the disease-related gene in a large consanguineous family. A novel missense mutation, p.Gly257Arg in *ERCC8*, was found to co-segregate with progressive spinocerebellar ataxia, skin photosensitivity, and intellectual disability.

Homozygosity mapping, haplotype analysis in the candidate regions, and whole exome sequencing were conducted to identify the disease-causing gene and mutation responsible for this apparently novel rare autosomal recessive disease [13,14]. In our study, five chromosomal segments were revealed by genome-wide linkage analysis and homozygosity mapping. High-resolution haplotype analysis confirmed the region 5q11.2-q13.2. Whole exome sequencing is a powerful tool for detecting disease-causing mutations. However, remains challenging to identify pathogenic mutations from among big data. Limiting our screening to the shared homozygosity region enabled us rule out most of the detected variants. Further data filtering for only coding homozygous variants led us to a single variant that was later confirmed by Sanger sequencing. The *ERCC8* mutation p.Gly257Arg is the only homozygous mutation within the homozygosity interval 5q11.2-q13.2. This mutation co-segregated with the disease phenotype within the family. It was not found as a polymorphic variant in publicly available databases or in the ethnic population and it affects an evolutionarily highly conserved amino acid. Extensive protein modelling clearly indicated that the mutation interferes with the normal function of the CSA protein. Combined homozygosity mapping and whole exome sequencing are promising, highly accurate, and affordable methods for identifying genetic defects in consanguineous families.

ERCC8 is located on chromosome 5q12.1, encoding CSA with a weight of 44 kD. CSA is a 396-amino acid polypeptide containing seven predicted WD40 repeat motifs. CSA interacts with CSB to recruit other repair factors to the site of UV-generated DNA damage [15,16]. Since *ERCC8* was cloned by Henning et al. in 1995 [16], approximately 58 different mutations have been reported in patients with CS-A and UVSS-2 [9,17,18].

CS-A is a developmental multisystem disorder with a heterogeneous clinical phenotype [6]. Three main factors are used to diagnose typical CS-A: growth failure, microcephaly, and developmental delay. The other clinical features include bilateral deafness, skin photosensitivity, intention tremor, arthrogryposis, progressive body fat loss, dental anomalies, cataracts, or characteristic facial features. CS-A has a continuous spectrum of severity, which can be divided into five subtypes: UVSS, late-onset type, classical type, early-onset type, and Cerebro-oculofacio-skeletal syndrome [19,20]. There is no clear threshold between the largely overlapping subgroups. In our study, the clinical symptoms of the proband were mild and unfeatured, including early-onset of cutaneous photosensitivity, mild intellectual disability, and late-onset ataxia. Thus, the diagnosis was not immediately established.

Combined homozygosity mapping and whole exome sequencing identified the pathogenic mutation p.Gly257Arg in this family. Fifty-eight pathogenic *ERCC8* mutations (including p.Gly257Arg) have been reported in different ethnic populations, including 24 point mutations (missense and nonsense mutations), 16 splicing mutations, 9 small deletions mutations, 4 small insertion mutations, 1 small indel mutation, 2 gross deletions, and 2 complex rearrangement mutations, which are summarized in Fig. 4 [8,10,12,21]. Single-nucleotide variants account for 68.97% (40/58) of *ERCC8* mutations. CSA is a highly conserved protein in vertebrates. These known disease-causing mutations are thought to abolish CSA function by disturbing WD40 repeat motifs. In our patients, p.Gly257Arg was located in the WD-5, which has a particularly high concentration of missense mutations. The missense mutations occur at evolutionarily conserved amino-acid residues in WD40 repeat motifs. Nonsense mutations are predicted to result in truncated CSA proteins lacking at least one WD40 repeat. Deletions, insertions, rearrangements, and splicing mutations are also located in the WD40 repeats. The motifs are required for the construction of the beta-propeller structure, which is important for protein complex formation and other protein-protein interactions. Thus, mutations at these positions can alter the protein's structure and thereby affect its associations with other proteins.

No obvious genotype-phenotype correlation was identified in previously reported CS-A patients [10]. Here, we reviewed *ERCC8* mutations and the clinical features of the continuous CS-A subtypes. Focusing on the homozygous CS-A patients, missense mutations appear to be more frequently associated with mild phenotypes than with protein-truncating mutations. Notably, the Trp361Cys mutation was identified in a patient with UVSS-2 [17]. Trp361 is a conserved residue located at WD-7, which interferes with transcription-coupled nucleotide excision repair (NER) but not with the oxidative stress response. This observation strongly supports that the severity of clinical features is related to the effects of the mutation on the additional roles of CSA outside transcription-coupled NER, which includes the oxidative damage response, mitochondrial function maintenance, and ribosomal DNA transcription [6,22]. Here, in our atypical CS-A patients, the Gly257Arg mutation may also have less effects on the additional roles of CSA, except for transcription-coupled NER. However, most *ERCC8* mutations were reported in typical CS-A patients. Thus, as recently summarized by Calmels et al. [10], patients with CS-A are more likely to fall into the type I category.

The NER pathway, which is a highly evolutionarily conserved repair mechanism, is one of the predominant, and perhaps universal, mechanisms contributing to the preservation of genomic integrity [23]. The mechanism of preferential recognition and correction of lesion in a gene being transcribed was not previously fully understood. A damage recognition factor in NER, Xeroderma pigmentosum complementation group C protein, is essential for this alternative NER pathway [24]. Notably, CSA plays an important role in this activity.

Taken together, these data highlight the importance of the novel *ERCC8* mutation p.Gly257Arg in the pathogenesis of atypical CS. Our results extended the mutation spectrum of *ERCC8* and illustrate the genotype-phenotype correlations in *ERCC8*-mutated patients. Further functional studies of these specific gene variants are needed to gain insight into the pathogenic mechanism(s). We also demonstrated that the combined strategy of linkage analysis and exome sequencing is useful for identifying disease-causing mutations.

Supplementary data to this article can be found online at https://doi.org/10.1016/j.cca.2019.03.1609.

Conflict of interest

The authors declare that they have no competing interests.

Acknowledgments

We would like to thank the family members for participating in this study. Consent for publication was obtained from the participants. This work was supported by National Natural Science Foundation of China (No.81570217), Natural Science Foundation of Chongqing (cstc2014jcyjA10074 and cstc2018jcyjAX0641), Fundamental Research Funds of Chongqing Population and Family Planning Science and Technology Research Institute (1612, 1603) and Foundation of Chongqing Health Commission (no. 2017MSXM069).

References

[1] M. Rossi, M. Anheim, A. Durr, C. Klein, M. Koenig, M. Synofzik, C. Marras, B.P. van de Warrenburg, P. International, C. Movement Disorder Society Task Force on, D. Nomenclature of Genetic Movement, The genetic nomenclature of recessive cerebellar ataxias, Mov. Disord. 33 (7) (2018) 1056–1076.

[2] T. Kawarai, A. Tajima, Y. Kuroda, N. Saji, A. Orlacchio, H. Terasawa, H. Shimizu, Y. Kita, Y. Izumi, T. Mitsui, I. Imoto, R. Kaji, A homozygous mutation of VWA3B causes cerebellar ataxia with intellectual disability, J. Neurol. Neurosurg. Psychiatry 87 (6) (2016) 656–662.

[3] W.M. Schmidt, S.L. Rutledge, R. Schule, B. Mayerhofer, S. Zuchner, E. Boltshauser, R.E. Bittner, Disruptive SCYL1 mutations underlie a syndrome characterized by recurrent episodes of liver failure, peripheral neuropathy, cerebellar atrophy, and Ataxia, Am. J. Hum. Genet. 97 (6) (2015) 855–861.

[4] A.C. Thomas, H. Williams, N. Seto-Salvia, C. Bacchelli, D. Jenkins, M. O'Sullivan, K. Mengrelis, M. Ishida, L. Ocaka, E. Chanudet, C. James, F. Lescai, G. Anderson, D. Morrogh, M. Ryten, A.J. Duncan, Y.J. Pai, J.M. Saraiva, F. Ramos, B. Farren, D. Saunders, B. Vernay, P. Gissen, A. Straatmaan-Iwanowska, F. Baas, N.W. Wood, J. Hersheson, H. Houlden, J. Hurst, R. Scott, M. Bitner-Glindzicz, G.E. Moore, S.B. Sousa, P. Stanier, Mutations in SNX14 cause a distinctive autosomal-recessive cerebellar ataxia and intellectual disability syndrome, Am. J. Hum. Genet. 95 (5) (2014) 611–621.

[5] V. Natale, H. Raquer, Xeroderma pigmentosum-Cockayne syndrome complex, Orphanet J. Rare Dis. 12 (1) (2017) 65.

[6] A.C. Karikkineth, M. Scheibye-Knudsen, E. Fivenson, D.L. Croteau, V.A. Bohr, Cockayne syndrome: clinical features, model systems and pathways, Ageing Res. Rev. 33 (2017) 3–17.

[7] A.M. Sijbers, P.C. van Voorst Vader, J.W. Snoek, A. Raams, N.G. Jaspers, W.J. Kleijer, Homozygous R788W point mutation in the XPF gene of a patient with xeroderma pigmentosum and late-onset neurologic disease, J. Invest. Dermatol. 110 (5) (1998) 832–836.

[8] N. Calmels, G. Greff, C. Obringer, N. Kempf, C. Gasnier, J. Tarabeux, M. Miguet, G. Baujat, D. Bessis, P. Bretones, A. Cavau, B. Digeon, M. Doco-Fenzy, B. Doray, F. Feillet, J. Gardeazabal, B. Gener, S. Julia, I. Llano-Rivas, A. Mazur, C. Michot, F. Renaldo-Robin, M. Rossi, P. Sabouraud, B. Keren, C. Depienne, J. Muller, J.L. Mandel, V. Laugel, Uncommon nucleotide excision repair phenotypes revealed by targeted high-throughput sequencing, Orphanet. J. Rare Dis. 11 (2016) 26.

[9] K. Kashiyama, Y. Nakazawa, D.T. Pilz, C. Guo, M. Shimada, K. Sasaki, H. Fawcett, J.F. Wing, S.O. Lewin, L. Carr, T.S. Li, K. Yoshiura, A. Utani, A. Hirano, S. Yamashita, D. Greenblatt, T. Nardo, M. Stefanini, D. McGibbon, R. Sarkany, H. Fassihi, Y. Takahashi, Y. Nagayama, N. Mitsutake, A.R. Lehmann, T. Ogi, Malfunction of nuclease ERCC1-XPF results in diverse clinical manifestations and causes Cockayne syndrome, xeroderma pigmentosum, and Fanconi anemia, Am. J. Hum. Genet. 92 (5) (2013) 807–819.

[10] N. Calmels, E. Botta, N. Jia, H. Fawcett, T. Nardo, Y. Nakazawa, M. Lanzafame, S. Moriwaki, K. Sugita, M. Kubota, C. Obringer, M.A. Spitz, M. Stefanini, V. Laugel, D. Orioli, T. Ogi, A.R. Lehmann, Functional and clinical relevance of novel mutations in a large cohort of patients with Cockayne syndrome, J. Med. Genet. 55 (5) (2018) 329–343.

[11] M. Khayat, H. Hardouf, J. Zlotogora, S.A. Shalev, High carriers frequency of an apparently ancient founder mutation p.Tyr322X in the ERCC8 gene responsible for Cockayne syndrome among Christian Arabs in northern Israel, Am. J. Med. Genet. A 152A (12) (2010) 3091–3094.

[12] X. Wang, Y. Huang, M. Yan, J. Li, C. Ding, H. Jin, F. Fang, Y. Yang, B. Wu, D. Chen, Molecular spectrum of excision repair cross-complementation group 8 gene defects in Chinese patients with Cockayne syndrome type a, Sci. Rep. 7 (1) (2017) 13686.

[13] H. Vahidnezhad, L. Youssefian, A. Jazayeri, J. Uitto, Research techniques made simple: genome-wide homozygosity/autozygosity mapping is a powerful tool for identifying candidate genes in autosomal recessive genetic diseases, J. Invest. Dermatol. 138 (9) (2018) 1893–1900.

[14] J. Gurgel-Giannetti, D.S. Lynch, A.R.B. Paiva, L.T. Lucato, G. Yamamoto, C. Thomsen, S. Basu, F. Freua, A.V. Giannetti, B.D.R. Assis, M.D.O. Ribeiro, I. Barcelos, K. Sayao Souza, F. Monti, U.S. Melo, S. Amorim, L.G.L. Silva, L.I. Macedo-Souza, A.M. Vianna-Morgante, M. Hirano, M.S. Van der Knaap, R. Lill, M. Vainzof, A. Oldfors, H. Houlden, F. Kok, A novel complex neurological phenotype due to a homozygous mutation in FDX2, Brain 141 (8) (2018) 2289–2298.

[15] S. Koch, O. Garcia Gonzalez, R. Assfalg, A. Schelling, P. Schafer, K. Scharffetter-Kochanek, S. Iben, Cockayne syndrome protein a is a transcription factor of RNA polymerase I and stimulates ribosomal biogenesis and growth, Cell Cycle 13 (13) (2014) 2029–2037.

[16] K.A. Henning, L. Li, N. Iyer, L.D. McDaniel, M.S. Reagan, R. Legerski, R.A. Schultz,

M. Stefanini, A.R. Lehmann, L.V. Mayne, E.C. Friedberg, The Cockayne syndrome group a gene encodes a WD repeat protein that interacts with CSB protein and a subunit of RNA polymerase II TFIIH, Cell 82 (4) (1995) 555–564.
[17] T. Nardo, R. Oneda, G. Spivak, B. Vaz, L. Mortier, P. Thomas, D. Orioli, V. Laugel, A. Stary, P.C. Hanawalt, A. Sarasin, M. Stefanini, A UV-sensitive syndrome patient with a specific CSA mutation reveals separable roles for CSA in response to UV and oxidative DNA damage, Proc. Natl. Acad. Sci. U. S. A. 106 (15) (2009) 6209–6214.
[18] V. Laugel, C. Dalloz, M. Durand, F. Sauvanaud, U. Kristensen, M.C. Vincent, L. Pasquier, S. Odent, V. Cormier-Daire, B. Gener, E.S. Tobias, J.L. Tolmie, D. Martin-Coignard, V. Drouin-Garraud, D. Heron, H. Journel, E. Raffo, J. Vigneron, S. Lyonnet, V. Murday, D. Gubser-Mercati, B. Funalot, L. Brueton, J. Sanchez Del Pozo, E. Munoz, A.R. Gennery, M. Salih, M. Noruzinia, K. Prescott, L. Ramos, Z. Stark, K. Fieggen, B. Chabrol, P. Sarda, P. Edery, A. Bloch-Zupan, H. Fawcett, D. Pham, J.M. Egly, A.R. Lehmann, A. Sarasin, H. Dollfus, Mutation update for the CSB/ERCC6 and CSA/ERCC8 genes involved in Cockayne syndrome, Hum. Mutat. 31 (2) (2010) 113–126.
[19] V. Laugel, Cockayne syndrome: the expanding clinical and mutational spectrum, Mech. Ageing Dev. 134 (5–6) (2013) 161–170.
[20] V. Natale, A comprehensive description of the severity groups in Cockayne syndrome, Am. J. Med. Genet. A 155A (5) (2011) 1081–1095.
[21] H. Xie, X. Li, J. Peng, Q. Chen, Z. Gao, X. Song, W. Li, J. Xiao, C. Li, T. Zhang, J.F. Gusella, J. Zhong, X. Chen, A complex intragenic rearrangement of ERCC8 in Chinese siblings with Cockayne syndrome, Sci. Rep. 7 (2017) 44271.
[22] M. Saijo, The role of Cockayne syndrome group a (CSA) protein in transcription-coupled nucleotide excision repair, Mech. Ageing Dev. 134 (5–6) (2013) 196–201.
[23] J.R. Portman, T.R. Strick, Transcription-coupled repair and complex biology, J. Mol. Biol. 430 (22) (2018) 4496–4512.
[24] S.M. Shell, E.K. Hawkins, M.S. Tsai, A.S. Hlaing, C.J. Rizzo, W.J. Chazin, Xeroderma pigmentosum complementation group C protein (XPC) serves as a general sensor of damaged DNA, DNA Repair (Amst) 12 (11) (2013) 947–953.